STEEL TUBE INSTITUTE

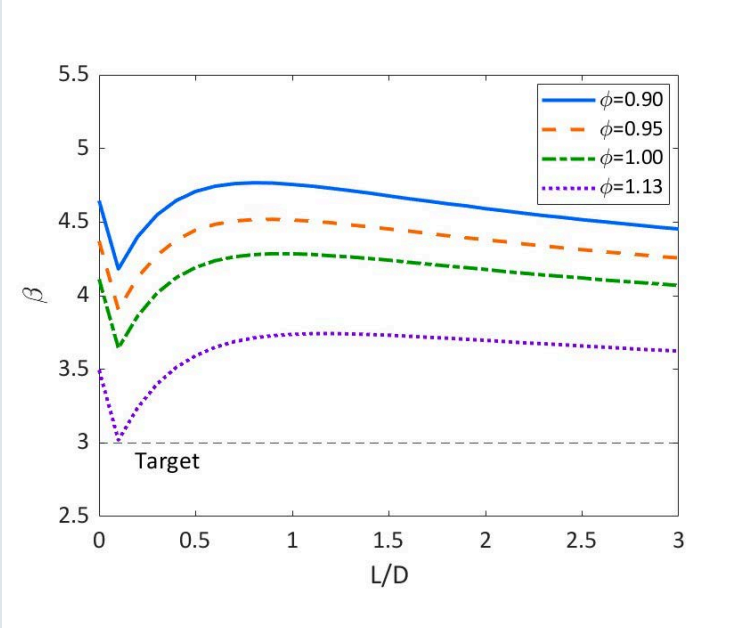

TRANSVERSE ELEMENTS-TO-HSS:

RELIABILITY OF THE PLATE LOCAL YIELDING LIMIT STATE

Jeffrey A. Packer
Department of Civil & Mineral Engineering, University of Toronto, Ontario, Canada

Ian G. Kennedy
Department of Civil & Mineral Engineering, University of Toronto, Ontario, Canada

TRANSVERSE ELEMENTS-TO-HSS: RELIABILITY OF THE PLATE LOCAL YIELDING LIMIT STATE

Jeffrey A. Packer

Department of Civil & Mineral Engineering, University of Toronto, Ontario, Canada

with Ian G. Kennedy

Department of Civil & Mineral Engineering, University of Toronto, Ontario, Canada

A transverse element, welded to the face of a rectangular HSS member, may arise in a transverse plate-to-HSS connection (Figure 1(a)) or an HSS-to-HSS gapped or overlapped K-connection (Figure 1(b)). In the latter, the "transverse element" is the wall of a branch member that is transverse to the HSS member on which it sits. Thus, in Figure 1(b), wall ***i*** of the overlapping branch is the transverse element that sits on transverse wall ***j*** of the overlapped branch.

(a) Transverse plate welded to HSS column

(b) Branch transverse wall-to-HSS overlapped branch

FIGURE 1

Examples of transverse elements welded to an HSS

The design of transverse plate-to-HSS welded connections is covered by Chapters J and K of the AISC 360 *Specification* (AISC, 2022), with elaboration in Part 9 of the AISC *Manual* (AISC, 2023). The pertinent limit states are, however, more clearly displayed in AISC *Design Guide 24* (DG24) (Packer and Olson, 2024), and are reproduced in Table 1. Limit states 4, 5 and 6, in that table, apply when the ratio of the width of the branch (plate) is approximately matched to the width of the chord, or $\beta \sim 1.0$. Usually the plate is sized to fit on the chord flat connecting face ($\beta < 1.0$) and then, for limit states 1, 2 and 3, it has been shown that limit state 3 (local yielding of the branch plate) theoretically governs over limit states 1 and 2, according to the simple nominal strength formulas (Packer, 2015; Packer and Olson, 2024). The local yielding limit state for transverse plates (or plate-like elements), highlighted in Table 1, is expressed by Eq. (K1-1) in the AISC *Specification* (AISC, 2022) in the format of a transverse element effective width (B_e). The importance of this transverse element local yielding limit state is such that it appears in the limit

states applied to T-, Y-, Cross and gapped/overlapped K-connections involving rectangular HSS (Packer and Olson 2024).

The purpose of this article is to delve into the background to this plate local yielding limit state, and to investigate the reliability of the assigned available strength by using contemporary best-practice structural reliability methods. As one can see in Table 1, the limit state nominal strength formula in question has a LRFD resistance factor (φ) of 0.95, whereas – being a yielding element in tension or compression – one might expect a resistance factor of 0.90 per AISC *Specification* Section J4.1 or Section J4.4 (AISC, 2022).

Table 1: Limit States for Transverse Plate-to-HSS Welded Connections (Packer and Olson, 2024)

Table 8-2. Available Strengths of Plate-to-Rectangular HSS Connections			
Connection Type	**Connection Available Strength[1]**	**Plate Bending[2]**	
	Plate Axial Load	**In-Plane**	**Out-of-Plane**
	Limit State 1: HSS plastification		
Transverse plate T- and cross-connections 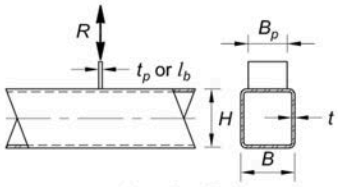 where $B_b = B_p$ and $\beta = B_b/B$ or B_p/B	$R_n = F_y t^2 \left[\frac{2t_p/B}{1-\beta} + \frac{4}{\sqrt{1-\beta}}\right] Q_f$ (2-2)	0	$M_n = F_y t^2 [X+Y] Q_f$ $X = \frac{0.5t_p(1+\beta)}{1-\beta}$ $Y = \sqrt{\frac{2BB_b(1+\beta)}{1-\beta}}$ (2-8)
	$\phi = 1.00$ (LRFD)	$\Omega = 1.50$ (ASD)	
	Limit State 2: HSS shear yielding (punching shear)		
	$R_n = 0.6F_y t(2t_p + 2B_{ep})$ $B_{ep} = \left(\frac{10t}{B}\right) B_b \le B_b$ (J4-3), (K1-2), (2-11), and (8-3a)	0	—
	$\phi = 1.00$ (LRFD)	$\Omega = 1.50$ (ASD)	
	Limit State 3: Local yielding of the branch plate		
	$R_n = \left(\frac{10t}{B}\right) F_y t B_b \le F_{yp} t_p B_b$ (K1-1), (2-14), (8-2a)	0	—
	$\phi = 0.95$ (LRFD)	$\Omega = 1.58$ (ASD)	
	Limit State 4: Local yielding of the HSS sidewalls		
	$R_n = 2F_y t(7.5t + t_p)$ (J10-2), (2-17)	0	$M_n = 0.5(B-t)R_n$
	$\phi = 1.00$ (LRFD)	$\Omega = 1.50$ (ASD)	
	Limit State 5: Local crippling of the HSS sidewalls		
	$R_n = 1.6t^2 \left(1 + \frac{3t_p}{H}\right) \sqrt{EF_y} Q_f$ (J10-4), (2-19)	0	—
	$\phi = 0.75$ (LRFD)	$\Omega = 2.00$ (ASD)	
	Limit State 6: Buckling of the HSS sidewalls		
	$R_n = \left(\frac{48t^3}{H-3t}\right) \sqrt{EF_y} Q_f$ (J10-8), (2-23)	0	—
	$\phi = 0.90$ (LRFD)	$\Omega = 1.67$ (ASD)	

BACKGROUND AND AVAILABLE DATA

A series of transverse plate-to-HSS connection tests was performed in The Netherlands more than 45 years ago (Wardenier et al., 1981), using low-strength, hot-formed hollow sections. That research produced plate effective width expressions for B_e and B_{ep}, Eqs. (K1-1) and (K1-2) respectively in the AISC

360 *Specification*, with one difference – the constant in the equations was 13.5, rather than 10 (which can be seen in equations for limit states 2 and 3 in Table 1). Over time, this constant of 13.5 has been rationalized downwards, to 11.7 for Grade 50 HSS (Davies and Packer, 1982), and lower still in order to provide sufficient "safety". In the first edition of CIDECT Design Guide No. 3 on rectangular HSS connections (Packer et al., 1992) this constant was 10, and has remained at this value to the most-recent technical publication on this topic (CEN, 2024), with an implied resistance factor of 1.0. The available database for transverse plate-to-rectangular HSS connections is shown in Table 2, which is augmented through the inclusion of additional experiments and numerical studies (Lu et al., 1993).

Table 2: Measured Properties of Experimental and Numerical Connection Specimens

Source	Specimen	B (in.)	t (in.)	B_p (in.)	t_p (in.)	F_y (ksi)	F_{yp} (ksi)
Wardenier et al. (1981)	P-1	7.15	0.246	7.16	0.254	48.7	38.0
	P-2	7.13	0.242	6.36	0.254	48.7	38.0
	P-3	7.14	0.238	5.56	0.254	48.7	38.0
	P-4	7.13	0.238	4.35	0.254	48.7	38.0
	P-5	7.18	0.369	6.35	0.361	37.6	40.9
	P-5-2	7.17	0.361	6.35	0.361	37.6	40.9
	P-6	7.18	0.357	5.56	0.357	37.6	40.9
	P-7	7.17	0.357	4.37	0.357	37.6	40.9
	P-8	7.17	0.532	6.35	0.476	36.8	31.8
	P-9	7.18	0.528	5.56	0.476	36.8	31.8
	P-10	7.18	0.532	4.37	0.476	36.8	31.8
	P-2-II	7.15	0.238	6.35	0.254	48.7	38.0
	P-4-II	7.17	0.242	4.37	0.258	48.7	38.0
	P-7-II	7.18	0.361	4.37	0.361	37.6	40.9
	P-8-II	7.18	0.536	6.36	0.468	36.8	31.8
	P-10-II	7.17	0.532	4.37	0.480	36.8	31.8
Lu et al. (1993)	1R1	11.9	0.390	4.75	0.392	62.9	57.7
	1R3	11.9	0.390	6.75	0.458	62.9	56.9
	xp1	11.9	0.754	3.61	0.317	51.5	100
	xp2	11.9	0.476	3.61	0.317	51.5	100
	xp3	11.9	0.317	3.61	0.317	51.5	100
	xp4	11.9	0.754	5.95	0.425	51.5	100
	xp5	11.9	0.476	5.95	0.425	51.5	100
	xp6	11.9	0.317	5.95	0.425	51.5	100
	xp7	11.9	0.754	8.73	0.754	51.5	100
	xp8	11.9	0.476	8.73	0.754	51.5	100
	xp9	11.9	0.317	8.73	0.754	51.5	100
	xp10	11.9	0.754	11.1	0.516	51.5	100
	xp11	11.9	0.476	11.1	0.516	51.5	100
	xp12	11.9	0.317	11.1	0.516	51.5	100

Table 3 provides the results of the experimental/numerical tests (T_{nx}) for the specimens listed in Table 2. To investigate the reliability of the plate local yielding limit state expression, specimens that failed in this manner must be identified. Neither Wardenier et al. (1981) nor Lu et al. (1993) explicitly state the failure

mode of individual specimens, though recorded experimental observations can be used to identify instances of weld failure or tube tearing. The characterization of other specimens is done by analyzing the force-displacement behavior of each test. If the transverse plate element fails by local yielding, the experimental data will show a distinct peak load, after which the force decreases. Conversely, specimens experiencing chord plastification (limit state 1 in Table 1) will not exhibit a peak load, as large displacements will be supported before an eventual strength plateau is reached. The ascertained failure modes are corroborated by the values of β in Table 3; chord plastification may govern when β is moderate to low (i.e., less than 0.75), whereas plate local yielding often governs when β is approximately equal to the width of the chord flat connecting face (which is often the prevalent case, see Figure 1(a)).

Table 3: Experimental/Numerical Specimen Capacities and Failure Modes

Source	Specimen	β	2γ	τ	T_{nx} (kips)	Failure mode
Wardenier et al. (1981)	P-1	1.00	29.0	1.03	42.0	Weld failure
	P-2	0.89	29.5	1.05	43.9	Plate local yielding
	P-3	0.78	30.0	1.07	26.8	Weld failure
	P-4	0.61	30.0	1.07	29.3	Chord tearing with weld failure
	P-5	0.88	19.5	0.98	58.5	Weld failure
	P-5-2	0.88	19.9	1.00	88.7	Plate local yielding
	P-6	0.77	20.1	1.00	48.6	Weld failure
	P-7	0.61	20.1	1.00	32.4	Weld failure
	P-8	0.88	13.5	0.90	122	Plate local yielding
	P-9	0.77	13.6	0.90	122	Plate local yielding
	P-10	0.61	13.5	0.90	71.7	Weld failure
	P-2-II	0.89	30.0	1.07	43.5	Plate local yielding
	P-4-II	0.61	29.6	1.07	29.6	Chord plastification
	P-7-II	0.61	19.9	1.00	52.5	Chord plastification
	P-8-II	0.89	13.4	0.87	133	Plate local yielding
	P-10-II	0.61	13.5	0.90	87.1	Plate local yielding
Lu et al. (1993)	1R1	0.40	30.0	1.00	38.8	Chord plastification
	1R3	0.57	30.0	1.20	52.9	Chord plastification
	xp1	0.30	15.8	0.42	107	Chord plastification
	xp2	0.30	25.0	0.67	40.8	Chord plastification
	xp3	0.30	37.5	1.00	18.6	Chord plastification
	xp4	0.50	15.8	0.49	148	Chord plastification
	xp5	0.50	25.0	0.89	54.6	Chord plastification
	xp6	0.50	37.5	1.34	24.9	Chord plastification
	xp7	0.73	15.8	1.00	249	Chord plastification
	xp8	0.73	25.0	1.58	89.4	Chord plastification
	xp9	0.73	37.5	2.37	40.6	Chord plastification
	xp10	0.93	15.8	0.68	337	Plate local yielding
	xp11	0.93	25.0	1.08	155	Plate local yielding
	xp12	0.93	37.5	1.62	78.3	Plate local yielding

RELIABILITY ANALYSIS

The reliability of the local yielding limit state expression in Table 1 can be investigated by calculating resistance factors using practical reliability assessment methods. Several methods are provided in different technical standards, though different underlying assumptions and simplifications often make it unclear which method should be used. Therefore, this article provides example calculations for three common methods. Based on the results of these analyses, the calculated resistance factors can be compared against the values that are currently recommended for design by DG24 (Packer and Olson, 2024) and the AISC *Specification* (2022). A comparison of the accuracy of different reliability assessment methods can also be made, to inform an optimised approach to calculating resistance factors that balances complexity and accuracy.

In LRFD, resistance factors are calculated to achieve a predetermined probability of failure. This is accomplished by using target reliability indices (β^+) as inputs within reliability assessment methods. Often, resistance factors will be calculated using a value of β^+ and then rounded downwards to a convenient number (e.g., 0.93 rounded to 0.90). This approach simplifies design and produces conservative solutions. Therefore, resistance factors used in design can be assigned any value less than or equal to the calculated magnitude, with a practical upper limit of $\varphi = 1.00$ for ultimate limit states. For the case of local yielding of transverse plate-to-HSS welded connections, a target reliability index of $\beta^+ = 3.0$ is used, as given by ASCE 7 (2022) for ductile failure modes.

Separation Factor Approach

The first method under investigation is known as the separation factor approach (SFA) and is recommended by ASCE 7 (2022). This approach has been used extensively to produce resistance factors since the origin of LRFD, though various technical standards provide different values of the separation factor (α_R). ASCE 7 (2022) suggests a value of 0.7, however the most used definition of α_R is 0.55 (Galambos and Ravindra, 1973). The SFA also requires the resistance bias coefficient (ρ_R) and coefficient of variation (CoV) (V_R), which account for the difference between the actual and nominal resistance. These parameters capture the variation in material and geometric variables, as well as the professional factor, which considers the variable accuracy of the nominal strength expressions. The resistance bias coefficient can be calculated as the product of the material, geometric, and professional factors, and the resistance CoV as the square root of the sum of the squares of the corresponding CoVs. Representative material and geometric statistics can be produced from experimental databases or found in the literature, whereas the professional factor and CoV are taken as the mean value and the CoV of the ratio of the experimental (or numerical) to nominal strengths. For the case of local yielding of transverse plate-to-HSS welded connections, the professional factor statistics are $\rho_P = 1.57$ and $V_P = 0.15$ and the material and geometric statistics are taken from the literature for ASTM A500 Grade B/C rectangular HSS and ASTM A572 Grade 50 plate: $\rho_M = 1.28$, $V_M = 0.09$, $\rho_G = 0.89$, and $V_G = 0.021$ (Schmidt and Bartlett, 2002; Liu et al., 2007; Liu, 2016). The resistance factor can then be calculated using the SFA, which gives a value of $\varphi = 1.34$.

$$\rho_R = \rho_M\,\rho_G\,\rho_P = (1.28)(0.89)(1.57) = 1.788$$

$$V_R = \sqrt{V_M^2 + V_G^2 + V_P^2} = \sqrt{(0.09)^2 + (0.021)^2 + (0.15)^2} = 0.176$$

$$\phi = \rho_R \exp\left(-\beta^+ \alpha_R V_R\right) = (1.788)\exp(-(3.0)(0.55)(0.176)) = 1.34$$

AISC 360-27 Appendix 9

An alternative reliability assessment method is presented in Appendix 9 of the forthcoming (2027) edition of the AISC *Specification*. This method is based on a similar approach provided in AISI S100 (2020), though statistical parameters including the calibration coefficient (C_φ = 1.48) and the CoV of the load effect (V_Q = 0.19) have been recalibrated for structural steel, as opposed to cold-formed (or light-gauge) steel. The 2027 *Specification* Appendix 9 method also uses material, geometric, and professional bias coefficients and CoVs, though values for these statistics are provided in Appendix 9, depending on the type of component and failure mode. For local yielding of transverse plate-to-HSS, statistics are taken for the case of "yielding in the connection elements", which gives the following parameters: ρ_M = 1.16, V_M = 0.10, ρ_G = 1.00, and V_G = 0.05 (AISC, 2025). This method also includes a sample size correction factor, to account for the inherent uncertainty when the database is small. Because only 10 experimental/numerical tests exist for the local yielding limit state (Table 3), it is expected that the sample size correction factor will have a non-negligible impact. The resistance factor can be calculated using the 2027 *Specification* Appendix 9 method, which gives a value of φ = 1.15.

$$C_n = \frac{n^2 - 1}{n^2 - 3n} = \frac{(10)^2 - 1}{(10)^2 - 3(10)} = 1.41$$

$$\phi = C_\phi\,\rho_M\,\rho_G\,\rho_P \exp\left(-\beta^+ \sqrt{V_M^2 + V_G^2 + C_n V_P^2 + V_Q^2}\right)$$

$$= (1.48)(1.16)(1.00)(1.57)\exp\left(-(3.0)\sqrt{(0.10)^2 + (0.05)^2 + (1.41)(0.15)^2 + (0.19)^2}\right) = 1.15$$

Approximate First-Order Reliability Method

The first-order reliability method (FORM) is another approach that has been used extensively in North America and is generally considered to be the most accurate closed-form reliability assessment method. This is a result of the FORM considering the variation in both the resistance and load variables, the latter of which is ignored in the SFA and simplified in the AISC 2027 *Specification* Appendix 9 method. An approximate FORM can be performed by assuming a governing load combination, which, for steel structures, is typically 1.2*D* + 1.6*L* from ASCE 7 (2022) (Ellingwood et al., 1980). Like the SFA, the FORM uses the bias coefficient and CoV of the resistance to account for material, geometric, and professional factor variation, so statistical parameters are identical to this approach. The calculation of the CoV of the loads (V_Q) and the resistance factor require bias coefficients and CoVs for the dead (*D*) and live (*L*) loads, which are taken as: ρ_D = 1.05, V_D = 0.10, ρ_L = 1.00, and V_L = 0.25 (Ellingwood and Culver, 1977; Ellingwood et al., 1980). Because the ratio of the live-to-dead loads (*L*/*D*) can vary, a conservative approach is to calculate resistance factors across the range of $0 \le L/D \le 3$ and select the minimum value. However, it is important to note that the principal dead load combination (1.4*D*) governs when *L*/*D* = 0.

The FORM can be used to calculate resistance factors for incremental values of *L/D*, which are listed in Table 4. From Table 4, a representative value of φ = 1.13 is selected.

Table 4: Resistance Factors Calculated Using the FORM, for Different *L/D*

L/D	V_Q	φ	*L/D*	V_Q	φ
0.0	0.10	1.30	1.6	0.18	1.20
0.1	0.10	1.16	1.7	0.18	1.19
0.2	0.10	1.19	1.8	0.19	1.19
0.3	0.10	1.22	1.9	0.19	1.18
0.4	0.11	1.23	2.0	0.20	1.18
0.5	0.11	1.24	2.1	0.20	1.17
0.6	0.12	1.24	2.2	0.20	1.17
0.7	0.13	1.24	2.3	0.21	1.16
0.8	0.13	1.24	2.4	0.21	1.16
0.9	0.14	1.23	2.5	0.21	1.15
1.0	0.15	1.23	2.6	0.21	1.15
1.1	0.15	1.22	2.7	0.22	1.14
1.2	0.16	1.22	2.8	0.22	1.14
1.3	0.17	1.21	2.9	0.22	1.14
1.4	0.17	1.21	**3.0**	**0.22**	**1.13**
1.5	0.18	1.20			

$$V_Q = \frac{\sqrt{(\rho_D V_D)^2 + (\rho_L V_L (L/D))^2}}{\rho_D + \rho_L (L/D)} = \frac{\sqrt{((1.05)(0.10))^2 + ((1.00)(0.25)(L/D))^2}}{(1.05) + (1.00)(L/D)}$$

$$\phi = \rho_R \left(\frac{\gamma_D + \gamma_L (L/D)}{\rho_D + \rho_L (L/D)} \right) \exp\left(-\beta^+ \sqrt{V_R^2 + V_Q^2} \right)$$

$$= (1.788) \left(\frac{(1.2) + (1.6)(L/D)}{(1.05) + (1.00)(L/D)} \right) \exp\left(-(3.0) \sqrt{(0.176)^2 + V_Q^2} \right)$$

Monte Carlo Simulation

In contrast to the previous closed-form reliability assessment methods, numerical approaches can be used to determine resistance factors with a high degree of accuracy, though they are often overly complex and time consuming for routine usage. Monte Carlo simulations (MCS) have been used historically for reliability analyses, as they can converge to the "exact" resistance factor. MCS operate by randomly sampling probabilistic distributions of all input parameters to calculate a sample resistance and load effect. When this is repeated many times over a range of representative connections, the probability of failure can be determined. Thus, MCS produce a distribution of the reliability index (β^+) over the range $0 \le L/D \le 3$ for each trial resistance factor under assessment. The exact solution is the trial resistance factor that exceeds the target reliability index over the full *L/D* range. For the case of local yielding of transverse plate-to-HSS welded connections, the likely exact resistance factor was

determined to be φ = 1.13 by preliminary approximate MCS. This is shown as the purple curve in Figure 2, plotted alongside the results for resistance factors of φ = 0.90, 0.95, and 1.00. The dip in reliability at *L/D* = 0.1 is produced due to the switch between the principal live and dead load combinations, which is seen to produce the minimum reliability for this case.

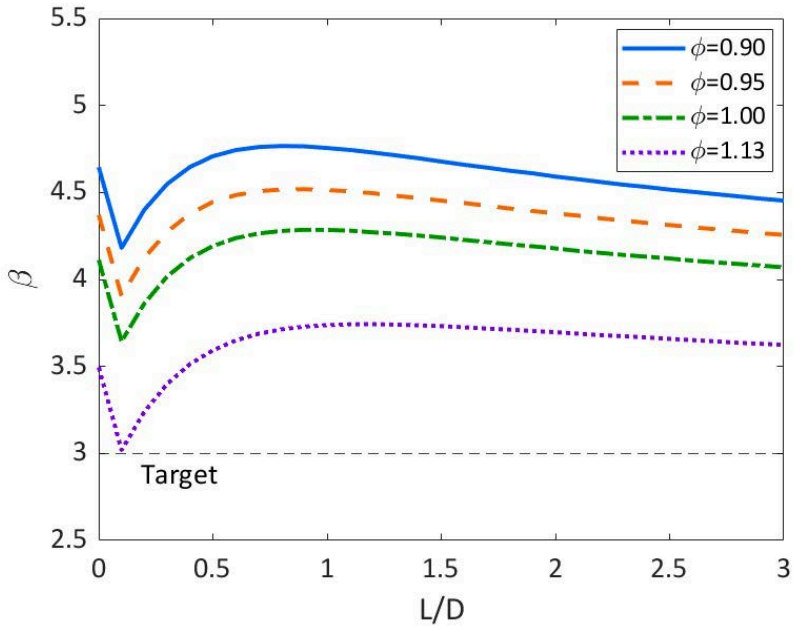

FIGURE 2

Reliability index distributions for trial resistance factors

CONCLUSION

Figure 2 shows that the exact resistance factor of φ = 1.13 is sufficient to meet the target reliability index of $\beta^+ = 3.0$, and that φ = 0.90, 0.95, and 1.00 all produce excessive reliability. Therefore, the use of a resistance factor of φ = 0.95 for the local yielding limit state of Table 1 provides adequate structural reliability. The primary reason for the magnitude of the exact resistance factor being much greater than typical values is the professional factor, which has a bias coefficient of $\rho_P = 1.57$ and a CoV of $V_P = 0.15$. These values indicate an overly conservative correlation between the nominal expression and the experimental/numerical test results. Given this poor correlation and the small experimental database, an opportunity for further research exists in the conduction of additional experimental/numerical tests and the derivation of a more-accurate nominal strength expression.

While the SFA, the 2027 AISC *Specification* Appendix 9, and FORM all predict resistance factors greater than 1.00, their results can be analyzed to determine the relative accuracies of each method. In comparison to the exact solution, the best prediction was provided by the FORM, followed by the 2027 AISC *Specification* Appendix 9 method, which was slightly unconservative. This is likely the result of using the statistical parameters given by Appendix 9 over the values from the literature used in the FORM. This

is confirmed by recalculating the resistance factor using the material and geometric statistics from the literature, which gives a value of φ = 1.13, equal to that of the FORM and the MCS. Conversely, the resistance factor produced by the SFA was unconservative and would produce unsafe solutions if used. This analysis shows that the FORM should be used to calculate resistance factors, though the 2027 AISC *Specification* Appendix 9 method can also provide accurate resistance factors if input statistics are fully representative of the limit state.

REFERENCES

AISC. 2022. "Specification for Structural Steel Buildings", ANSI/AISC 360–22, American Institute of Steel Construction, Chicago, IL.

AISC. 2023. "Steel Construction Manual", 16th edition, American Institute of Steel Construction, Chicago, IL.

AISC. 2025. "Specification for Structural Steel Buildings", 2nd Public Review Draft, ANSI/AISC 360–27, American Institute of Steel Construction, Chicago, IL.

AISI. 2020. "North American Specification for the Design of Cold-Formed Steel Structural Members", AISI S100-16 (2020), American Iron and Steel Institute, Washington, DC.

ASCE. 2022. "Minimum Design Loads and Associated Criteria for Buildings and Other Structures", ASCE/SEI 7-22, American Society of Civil Engineers, Reston, VA.

CEN. 2024. "Eurocode 3 – Design of Steel Structures – Part 1-8: Joints", EN 1993-1-8: 2024(E), European Committee for Standardization, Brussels, Belgium.

Davies, G. and Packer, J.A. 1982. "Predicting the Strength of Branch Plate – RHS Connections for Punching Shear", Canadian Journal of Civil Engineering, Vol. 9, No. 3, pp. 458-467.

Ellingwood, B. and Culver, C. 1977. "Analysis of Live Loads in Office Buildings", Journal of the Structural Division, Vol. 103, No. 8, pp. 1551-1560.

Ellingwood, B., Galambos, T.V., MacGregor, J.G. and Cornell, C.A. 1980. "Development of a Probability Based Load Criterion for American National Standard A58", NBS Special Publication 577, National Bureau of Standards, Gaithersburg, MD.

Galambos, T.V. and Ravindra, M.K. 1973. "Tentative Load and Resistance Factor Design Criteria for Steel Buildings", Research Report No. 18, Washington University in St. Louis, St. Louis, MO.

Liu, J. 2016. "Updates to Expected Yield Stress and Tensile Stress Ratios for Determination of Expected Member Capacity in the 2016 AISC Seismic Provisions", Engineering Journal, Vol. 53, No. 4, pp. 215-228.

Liu, J., Sabelli, R., Brockenbrough, R.L. and Fraser, T.P. 2007. "Expected Yield Stress and Tensile Strength Ratios for Determination of Expected Member Capacity in the 2005 AISC Seismic Provisions", Engineering Journal, Vol. 44, No. 1, pp. 15-26.

Lu, L.H., Puthli, R.S. and Wardenier, J. 1993. "Semi-Rigid Connections Between Plates and Rectangular Hollow Sections Columns", in Proceedings of 5th International Symposium on Tubular Structures, Nottingham, UK, pp. 723-731.

Packer, J.A. 2015. "Transverse Plate-to-Square/Rectangular HSS Connections", Steel Tube Institute HSS Technical Article, https://steeltubeinstitute.org/resources/transverse-plate-to-squarerectangular-hss-connections/

Packer, J.A. and Olson, K. 2024. "Hollow Structural Section Connections", Steel Design Guide No. 24, 2nd edition, American Institute of Steel Construction, Chicago, IL.

Packer, J.A., Wardenier, J., Kurobane, Y., Dutta, D. and Yeomans, N. 1992. "Design Guide for Rectangular Hollow Section (RHS) Joints under Predominantly Static Loading", CIDECT Design Guide No. 3, 1st edition, CIDECT and Verlag TÜV Rheinland, Köln, Germany.

Schmidt, B.J. and Bartlett, F.M. 2002. "Review of Resistance Factor for Steel: Data Collection", Canadian Journal of Civil Engineering, Vol. 29, No. 1, pp. 98-108.

Wardenier, J., Davies, G. and Stolle, P. 1981. "The Effective Width of Branch Plate to RHS Chord Connections in Cross Joints", Stevin Laboratory, Report No. 6-81-6, Delft University of Technology, Delft, The Netherlands.